 FDMP, vol.10, no.2, pp.241-260, 2014

Inclined Plane Jet Impinging a Moving Heated Wall

D. Benmouhoub[1] **and A. Mataoui**[1]

Abstract: The present work is devoted to the numerical study of the interaction of an inclined plane turbulent jet with a moving horizontal isothermal hot wall. The inclination of the jet allows the control of the stagnation point location. Numerical predictions based on statistical modeling are obtained using a second order Reynolds stress turbulence model coupled to an enhanced wall treatment. For a given impinging distance H (H =8e), the considered problem parameters are: (a) jet exit Reynolds number (Re, based on the thickness "e" of the nozzle) in the range from 10000 to 25000, (b) surface-to-jet velocity ratio Rsj from left to right; ranging between 0 and1.75 and (c) optimal inclination angle of the jet between 0° to 25°. The calculations are in good agreement with the available data. The numerical results show that the heat transfer is greatly influenced by the velocities of the jet and the moving wall. In particular, the local Nusselt number decreases with increasing surface-to-jet velocity ratios (until Rsj=1). Optimal inclination of the jet can be used to enhance heat transfer and modify the stagnation point location. The distribution of average Nusselt number is correlated with typical problem parameters.

Keywords: Impinging jet, inclined slot jet, fluid phenomena, heat transfer, Nusselt number, correlation.

Nomenclature

e	Nozzle width, [m]
H	Impinging distance, [m]
I	Turbulent intensity
k	Turbulent kinetic energy [m^2s^{-2}]
L	Length of the impingement plate, [m]
Nu_x	Local Nusselt number, [-]
$\overline{Nu}$	Average Nusselt number, [-]

[1] Laboratoire de mécanique des fluides théorique et appliquée, Faculté de physique, Université des Sciences et de la Technologie Houari Boumediene, B. P. 32, Bab Ezzouar, 16111 Al Alia, Alger, Algérie.

P Mean pressure, [Pa]
Re Reynolds number, [-]
R_{sj} Surface-to-jet velocity ratio, [-]
T Mean temperature, [K]
U Mean velocity in the x-direction, [ms^{-1}]
U_i Mean velocity components, [ms^{-1}]
u_j Fluctuating velocity components, [ms^{-1}]
V Mean velocity in the y-direction, [ms^{-1}]
V_{0j} Jet exit velocity exit, [ms^{-1}]
x Longitudinal coordinate [m]
x_i Coordinate directions, [m]
y^+ dimensionless distance to the nearest wall, [-]

Greek symbols

α Angle of inclination, [$^\circ$]
δ Gain of the stagnation Nusselt number
Δ Gain of the average Nusselt number
θ Fluctuating temperature [k]
ν Kinematic viscosity, [m^2s^{-1}]
ρ Fluid density, [Kgm^{-3}]

Subscripts

C cold temperature
H Hot temperature
in Inlet

1 Introduction

Impinging jets have several industrial applications including the tempering of glass plate, annealing of metal sheets, drying of textile and paper products. In these applications, the jet impinges a moving flat plat. Only few studies have reported the effect of the impingement surface motion on the flow field and the heat transfer. The first work of jet impingement on a moving wall is that of Subba Raju and Schlünder (1977). They have investigated experimentally heat transfer from a single jet on a moving belt. Huang et al. (1984) performed numerical modeling of a turbulent, plane air jet on a rectangular duct with surface motion effects. They found that

for a high speed of the plate, the Nusselt number is smaller than those at the areas are where movement of the surface is opposite to the jet flow, and increases in the region where the movement of the plate and flow are done in the same direction. Zumbrunnen et al. (1992) investigated analytically the case of a slot laminar jet, impinging an isothermal moving plate subjected to a constant flux.They showed that the heat transfer is more effective due to the slowdown of the development of the boundary layer away from the jet due to the effect of the plate motion. Chattopadhyay et al. (2002) examined numerically using Large Eddy Simulation (LES), the heat transfer of an array of plane jets impinging a moving plate; for a jet exit Reynolds number ranging between 500 and 3000 and for several surface-jet velocities ratios Rsj of: 0, 0.5, 1 and 2. They confirm that the distribution of the Nusselt number on the plate becomes uniform when the plate velocity decreases. Later, Chattopadhyay and Saha (2003) using large eddy simulation LES, studied the turbulent flow and heat transfer, generated by a single jet impinging a heated moving isotherm plate. They presented the results for only one Reynolds number of 5800, with a single perpendicular jet impinging a moving plate at surface-to-jet velocities ratios between 0 and 2. The normalized impinging distance was 10. They mainly focused on the details of the flow structure and the profiles of the velocity and those of the stresses .The confined flow field of a turbulent slot air jet impinging perpendicularly a flat plate, was investigated experimentally by Senter (2006). The experiments were conducted for a nozzle-to-plate spacing of 8 slot nozzle widths, for three Reynolds number (5300, 8000, and 10600) and four surface-to-jet velocity ratios (0, 0.25, 0.5 and 1.0). It appears that the flow patterns for a given surface-to-jet velocity ratio, are independent of the jet Reynolds number in the range of 5300–10600. A slight modification of the flow field occurs for the case of surface-to-jet velocity ratio of 0.25, but for higher ratios of 0.5 and 1, the streamlines are strongly deformed. At a given Reynolds number of 10600 and for normalized plate velocities 0, 0.25, 0.5 and 1.0. Senter (2006) has investigated numerically the local Nusselt number by the CFD code Fluent, using the k-ε WCP turbulence model. This study showed that the influence of the jet on the local Nusselt number around the impinging area. He found that local Nusselt number decreases significantly when the plate velocity increases. After that, Sharif et al. (2009) using CFD code Fluent, by means of the standard k - ε turbulence model coupled to enhanced wall treatment. They have shown that the local Nusselt number along the moving plate exceeds the values near of the impinging region for the low plate velocities, which are due to the thinning of dynamical and thermal boundary layers. These excess decreases for higher plate velocities, are due to the domination of the driven parallel flow by the plate motion. At a given plate velocity, the average Nusselt number increases while the average skin friction coefficient decreases when jet Reynolds number augments. On the other hand, at a given Reynolds number of 10600, both

of these quantities decrease slightly initially and then increase sharply for a faster plate velocity. By the RANS k-ω turbulence model, Benmouhoub and Mataoui (2013) investigated the turbulent flow and heat transfer of a plane jet impinging a moving hot wall, for a Reynolds number between 10000 and 25000, a nozzle to plate spacing of 8e, and velocity ratio ranging between 0 – 4. They presented correlation for average Nusselt number and average skin friction coefficient in terms of Reynolds number and surface-to-jet velocity ratio.

Korger and Kized (1972), Belataos (1976), Beitlmal et al. (2000), Tong (2003) and Ramzanpour (2007) examined the case of slot jet impinging an immobile inclined wall. They concluded that, the maximum transfer coefficients are highest for the case of perpendicular impingement. They also showed that the maximum heat transfer region (stagnation point) shifts towards the uphill side of the plate and the maximum Nusselt number value decreases as the inclination angle increases. Senter (2006), from measurements of the case of a perpendicular jet impingement on a mobile wall, examined the inclined case in order to recover the characteristics of perpendicular impingement on an immobile wall. Indeed, for a Reynolds number of 10600 and surface-to-jet velocity ratio of 1, Senter (2006) confirmed an improvement in the Nusselt average number of 25% for a jet inclination of 8°.

The present study extends the previous work of a perpendicular jet interaction on a moving wall by examining the effect of the jet inclination on the flow structure and heat transfer. The objective of this work is to find the inclination corresponding to the flow structure case of a jet impinging perpendicularly on an immobile wall.

2 Methodology

2.1 Governing equations

The flow is steady on average and fully turbulent. The fluid (air) is incompressible with constant thermo physical properties. The conservatives averaged equations are: mass (Eq. 1), momentum (Eq. 2) and energy (Eq. 3). These equations are coupled with the equations of the turbulence model:

$$\text{- Continuity} \quad \frac{\partial U_i}{\partial x_i} = 0 \tag{1}$$

$$\text{- Momentum} \quad U_j \frac{\partial U_i}{\partial x_j} = -\frac{\partial}{\partial x_i}\left(\frac{P}{\rho}\right) + \frac{\partial}{\partial x_j}\left(\nu \frac{\partial U_i}{\partial x_j} - \overline{u_i u_j}\right) \tag{2}$$

$$\text{- Energy} \quad U_i \frac{\partial T}{\partial x_i} = \frac{\partial}{\partial x_i}\left(\gamma \frac{\partial T}{\partial x_i} - \overline{u_i \theta}\right) \tag{3}$$

2.2 Turbulence Model

The closure of the averaged equations is achieved by linear strain pressure - Reynolds stress second order model. This model does not require eddy viscosity hypothesis. Six transport equations of each Reynolds stresses components ($\rho\overline{u_i u_j}$) are added to the averaged Equations ((1), (2) and (3)).The differential equation Reynolds stress transport consist of the standard Reynolds stress model based on dissipation equation ε. There are three versions of the standard Reynolds stress models. They are called: LRR-IP, LRR-QI and SSG. Launder, Reece and Rodi (1975) developed the LRR-IP and LRR-QI models. The pressure-strain expression consists of an anisotropy tensor, mean strain rate tensor and vorticity tensor. The production due to the buoyancy is neglected in this study. Rather significant viscosity effects characterize the flow close to the wall. Therefore, the high Reynolds models are no longer suitable any more in this area of flow. The wall treatment is required. After several tests, the enhanced wall treatment predicts the flow fields with the best accuracy [Kader (1981)].

2.3 Numerical procedure

The numerical predictions based on finite volume method are performed by ANSYS FLUENT 14.0 CFD code. The discretization of each transport equation is done on collocated meshes (ANSYS14 Documentation). The algorithm SIMPLEC is used for pressure-velocity coupling. The POWER LAW interpolation scheme is applied for the convection–diffusion interpolation terms of velocity components, temperature, Reynolds stress components and dissipation. For pressure a Second order scheme was adapted. As usual, the source terms in the turbulence equations are linearized to insure the stability of the solution.

2.3.1 Boundary conditions

Four types of boundary conditions were adapted to predict the flow field within the computational domain:

(a) *Air jet duct inlet:* The conditions at the jet exit boundary are important in predicting the evolution of the centerline velocity and shear stresses. A parabolic profile is used for the jet exit velocity [Senter (2006)]. It is expressed by:

$$V_j(x) = -V_{oj}\left(1-\left(\frac{|x|}{e/2}\right)^7\right) \text{ where } V_{oj} = \frac{\nu Re}{e} \tag{4}$$

Therefore, the velocity components, kinetic energy and dissipation rate are deduced from (Eq. 5):

$U(x) = V_j(x).\cos(\alpha), \quad V(x) = V_j(x).\sin(\alpha)$

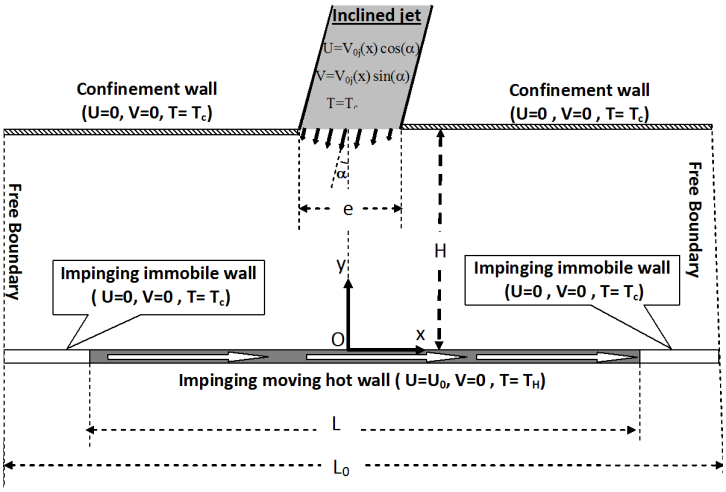

Figure 1: Configuration and boundary conditions.

$$k_{in} = I.(V_{0j})^2 \quad \text{where} \quad I = 0.02 \quad \text{and} \quad \varepsilon_{in} = C_\mu \frac{(k_{in})^{3/2}}{0.03e}$$

The jet exit is set at ambient temperature T_c of 293K.

(b) *Wall boundaries conditions:* U=V=0 wall are imposed for immobile walls. These walls are adiabatic. While the moving wall is subjected to a constant horizontal velocity U=U_0; V=0 and a hot temperature T_H of 313K ; $T_H > T_C$. As pointed out in part 2.2 on the wall effect on turbulence, an enhanced wall treatment and near wall modeling approaches were used [Kader (1981)].

(c) *Air exit boundary ($x = \pm L_0/2$):* The pressure outlet (fully developed) (boundary conditions were used at all exit boundary. The relative static pressure at these boundaries was set to zero; assumed the atmospheric pressure (reference pressure kept at atmospheric level).

2.3.2 Grid arrangement

A two dimensional structural non-uniform grid was generated. The enhanced wall treatment is used, which requires a fine grid size in the vicinity to the wall, requiring $y^+ < 3.5$ (Figure 2).

Several distributions of the grid were tested to examine their independence on the solution. Figure 3 shows the effect of cells size on the evolution of the local Nusselt number. It is noticed that the independence of the grid on the solution is obtained for 290×90 nodes beyond which no further significant change is observed. This

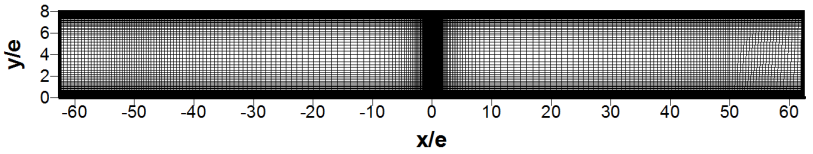

Figure 2: Typical grid arrangement.

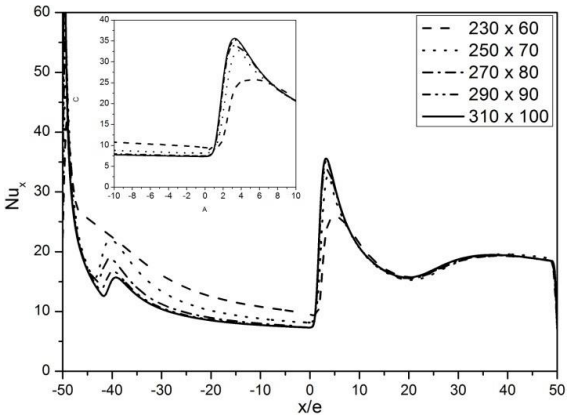

Figure 3: Effect of grid refinement on the local Nusselt number along the moving wall, Re=10000, Rsj=1, α=0, H/e=8.

grid distribution is therefore used in all subsequent calculations.

2.3.3 Validation

The validation of the numerical technique is checked on the dynamic and thermal fields. The normalized velocities (U/V_{0j}) and (V/V_{0j}) for two horizontal sections (y=0.3, and 4) for two cases: Rsj=0, α=0 and Rsj=1, α=9°, and Re=10600, were compared to PIV experimental data of Senter (2006) (Fig. 3). As shows Fig. 4, a good agreement was obtained. Figure (1) shows also a good agreement with the experimental data of Gardon and Akfirat (1966) for the case of an immobile wall corresponding to Rsj=0, α=0°, H/e=8 and Re=11000.

This numerical study is in good agreement with several previous works, therefore this grid can be used for other cases of interactions, because the geometrical characteristics (H, e, L and L_0) are kept constant in the whole study.

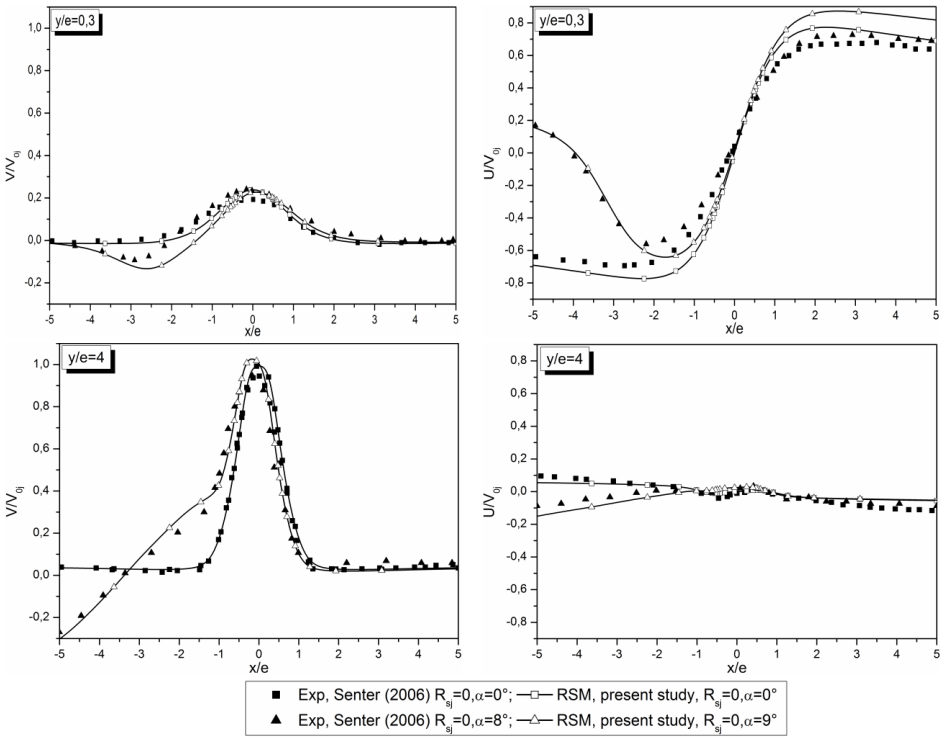

Figure 4: Mean velocity components U/V_{0j} and V/V_{0j}, Re=10600, for horizontal sections y/e=0.3 and 4.

3 Results and discussion

The numerical values of parameters in this study are given in the Table 1. As mentioned above, the numerical predictions are performed in order to investigate the influence of inclination of the jet on the streamlines and on Nusselt number evolution.

3.1 Mean flow structure

The mean flow structure is examined for the case Re=10600 and H/e=8. The streamlines contours are illustrated in Figs 6 - 9, for the cases of surface-to-jet velocities ratios of $0 \leq$ Rsj ≤ 1.75 and their corresponding inclined cases that allow obtaining the case of a jet impinging perpendicularly on a stationary wall ($0^\circ \leq \alpha \leq 25^\circ$). Figures 6 , 7 and 8 show a good agreement with PIV measurement [Senter (2006)] only for the cases where $R_{sj} \leq 1.0$

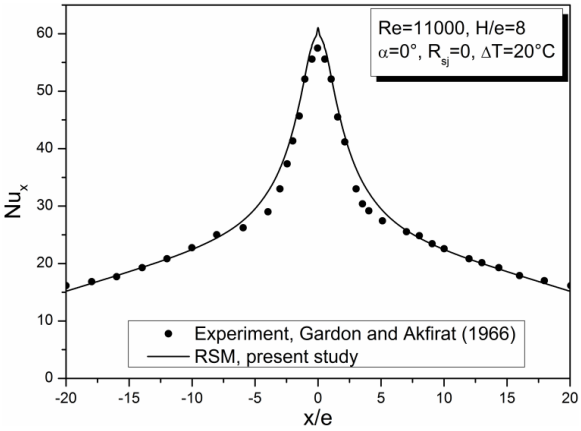

Figure 5: Comparison of local Nusselt number prediction with the experiment data of Gardon and Akfirat (1966).

Table 1: Test cases parameters.

e	H/e	L/e	L_0/e	α	R_{sj}	Re
0.02m	8	100	125	$0^{\circ} \leq \alpha \leq 25^{\circ}$	$0 \leq R_{sj} \leq 1.75$	$10000 \leq Re \leq 25000$

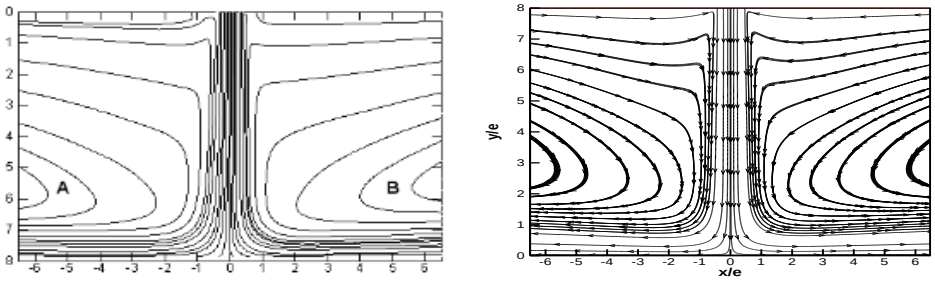

PIV, R_{sj}= 0, α=0° R_{sj}= 0, α=0°

Figure 6: Streamlines contours of jet impinging immobile wall, Re=10600.

For Rsj=0, α=0, corresponding to a turbulent slot impinging perpendicularly on an immobile plate, the flow topology is perfectly symmetric relative to the jet axis. Two identical vortices appear on either side of the nozzle generated by the driving of the flow and by the upper confinement wall effect (Fig. 6).

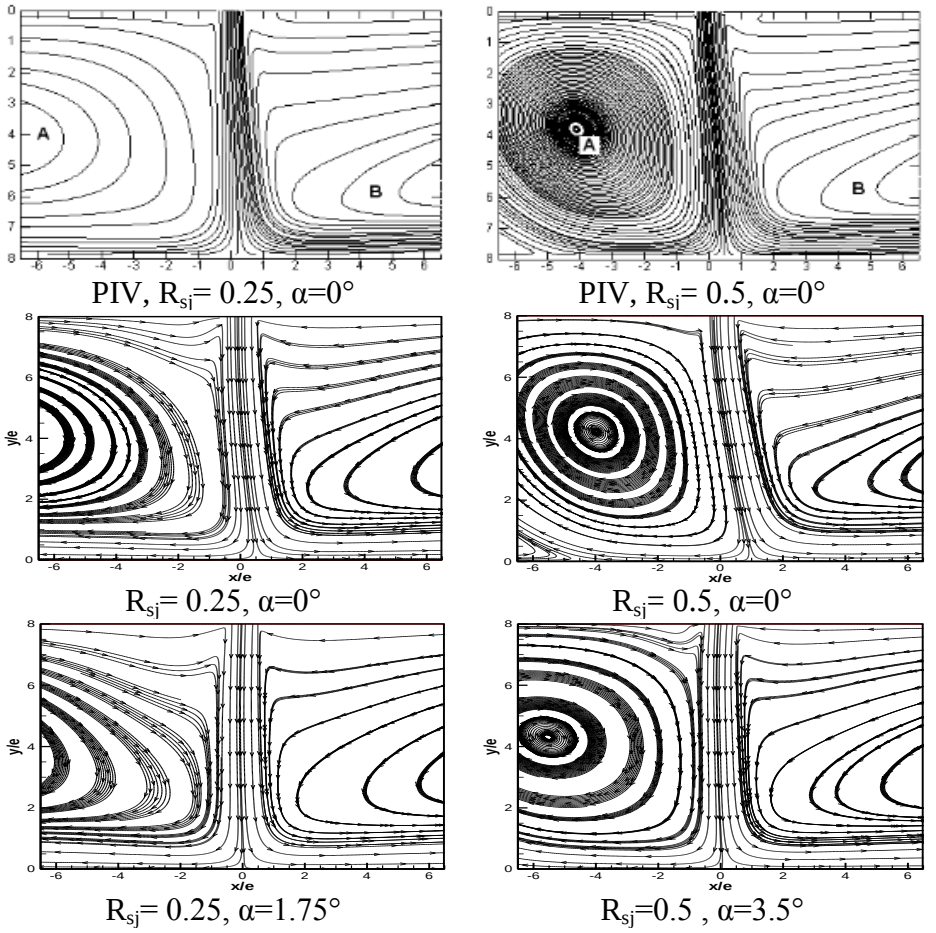

Figure 7: Streamlines contours: effect of surface-to-jet velocities ratio and inclination angle Re=10600, $0 < R_{sj} < 1$, $0^\circ \leq \alpha \leq 9^\circ$.

The first case ($R_{sj} < 1$) corresponds to a small wall velocity (Figure 7). The jet velocity is superior to that of the plate, inducing a stagnation zone and a new recirculation zone on the left side of the moving wall counter-rotating to the main vortex. The size of this new vortex increases when the surface-to-jet velocity ratio

augments, and compresses the left primary vortex, therefore the jet is gradually deviates to the right in the same direction as the moving wall [(Senter (2006), Sharif et al. (2009), Benmouhoub and Mataoui (2013)]. The location of the stagnation point is therefore shifted. The inclination allows retrieving the case of the jet impinging perpendicularly to a stationary wall. These inclinations are obtained by several tests.

When the wall moves from left to right, the flow is entrained to the right in the same direction, because of the additional shear of this type of flow pattern. The inclination of the nozzle modifies the flow structure in order to find the case of the interaction of a jet perpendicular to a fixed wall. Two ranges of surface-to-jet velocities ratios are examined: $R_{sj} < 1$ and $1 \leq R_{sj} \leq 1.75$.

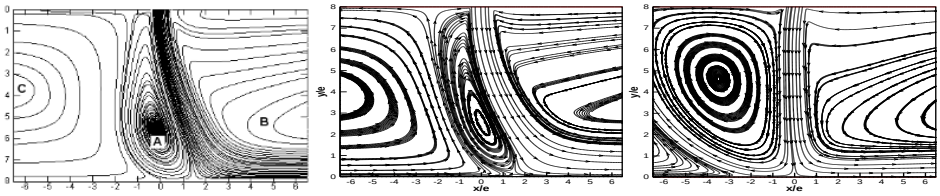

Experiment (PIV): α=0° Present study : α=0° Present study : α=9°

Figure 8: Streamlines contours: effect of surface-to-jet velocity ratio and inclination angle, Re=10600, R_{sj} =1 $\alpha = 9^{\circ}$.

For $R_{sj} \geq 1$ the jet is completely deviated by the movement of the wall. For no-inclined cases ($R_{sj} \geq 1$, α=0), the jet does not attain the moving wall and its streamlines become parallel progressively to the wall when the surface-to-jet velocities ratio increases. The shear drives the flow by the moving wall is much larger than that of that the left region. The inclined cases ($R_{sj} \geq 1$) have the same behavior for the non inclined case of R_{sj}=1. There are characterized by a small new recirculation at the left side of the jet as shown Figure 8 and Figure 9. As shown table 2, when the surface-to-jet velocities ratio increases, the inclination of the jet augments.

Table 2: surface-to-jet velocities ratio: effect on inclination.

R_{sj}	0	0.25	0.5	1	1.25	1.5	1.75
α	0°	1.75°	3.5°	9°	12°	17.75°	25°

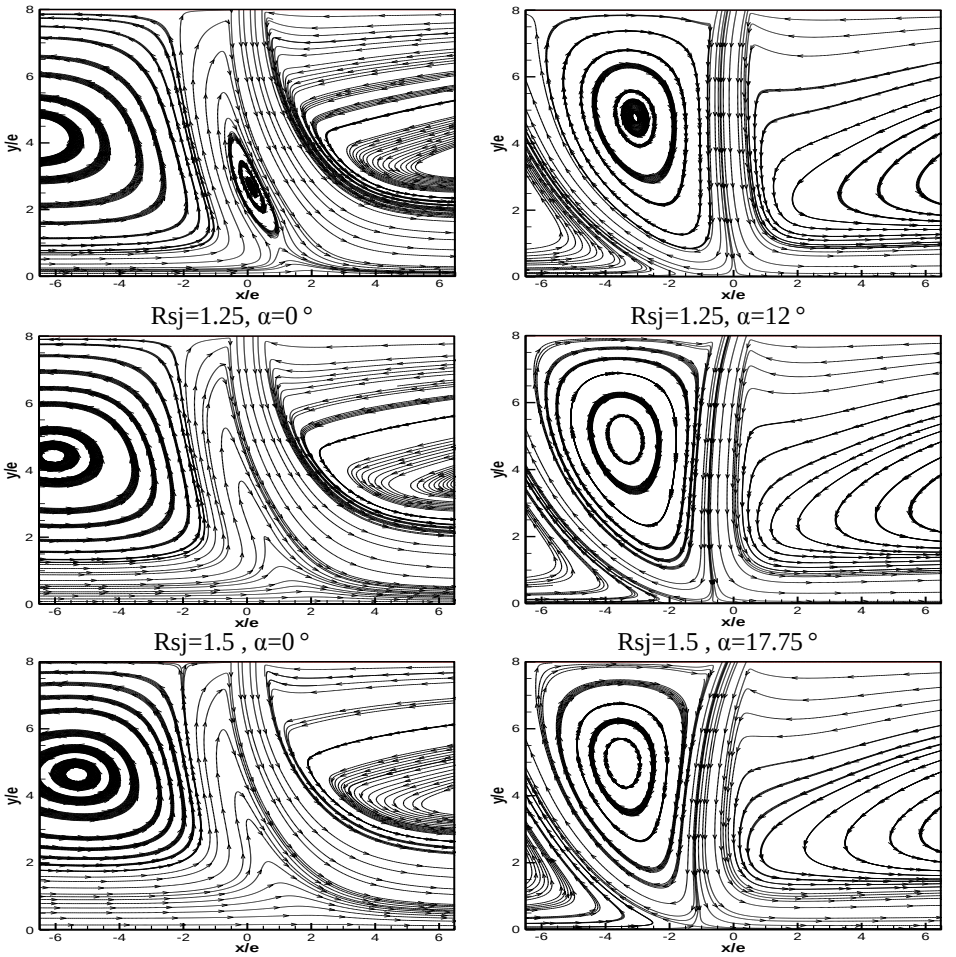

Figure 9: Streamlines contours: effect of surface-to-jet velocities ratio and inclination angle Re=10600, $1 < R_{sj} \leq 1.75$, $0^{\circ} \leq \alpha \leq 25^{\circ}$.

3.2 Heat transfer

3.2.1 Isotherms

Figure 10 shows the temperature contours for the non-inclined cases and inclined cases, simultaneously. The Solid lines represent non-inclined cases and dashed lines represent inclined cases. In the non inclined cases, for a large surface-to-jet velocities ratio, there is no stagnation region (Benmouhoub and Mataoui (2013));

the flow is completely deflected from the wall. The corresponding inclination of the jet; allows us to obtain the behaviour of the perpendicular jet impingement on an immobile wall. This figure confirms the existence of a stagnation point for each inclined case.

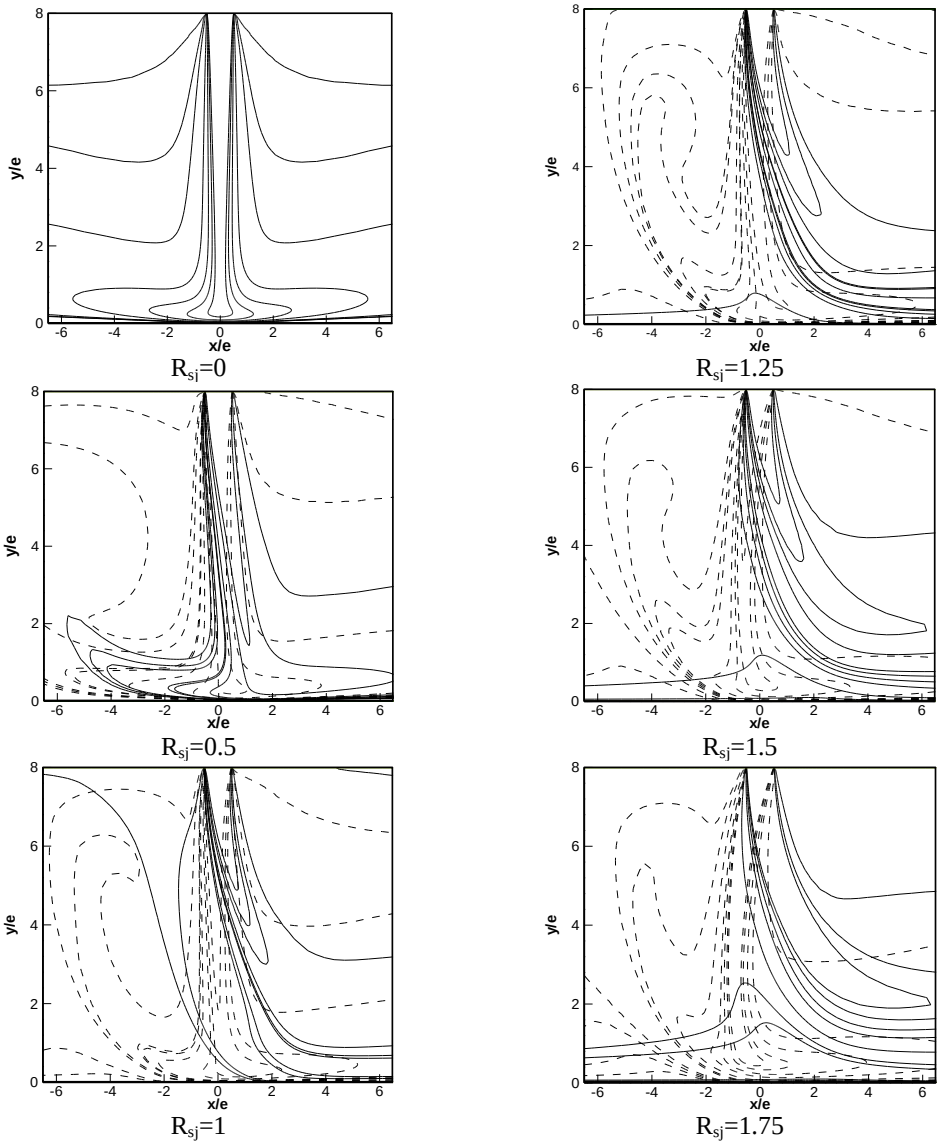

Figure 10: Temperature contours Re=10600, $0 < R_{sj} \leq 1.75$, $0^{\circ} \leq \alpha \leq 25^{\circ}$. Solid lines (non-inclined cases) and dashed lines (inclined cases)..

3.2.2 Nusselt number distribution

The dimensionless Nusselt number defines the heat transfer of fluid along the heated impinging wall, which characterizes the ratio of convective to conductive heat transfer across the corresponding wall boundary. The local Nusselt number distribution over the impingement wall is defined in Eq. 5:

$$Nu(x) = -\left(\frac{e}{T_H - T_C}\right)\left(\frac{\partial T}{\partial n}\right)_{ywall} \tag{5}$$

Where n is the perpendicular direction to the corresponding wall

The average Nusselt number along the moving wall is deduced from the following expression (Eq.6):

$$\overline{Nu} = \frac{1}{L}\int_{-L/2}^{L/2} Nu(x)dx \tag{6}$$

3.2.2.1 Effect of surface-to-jet velocities ratio

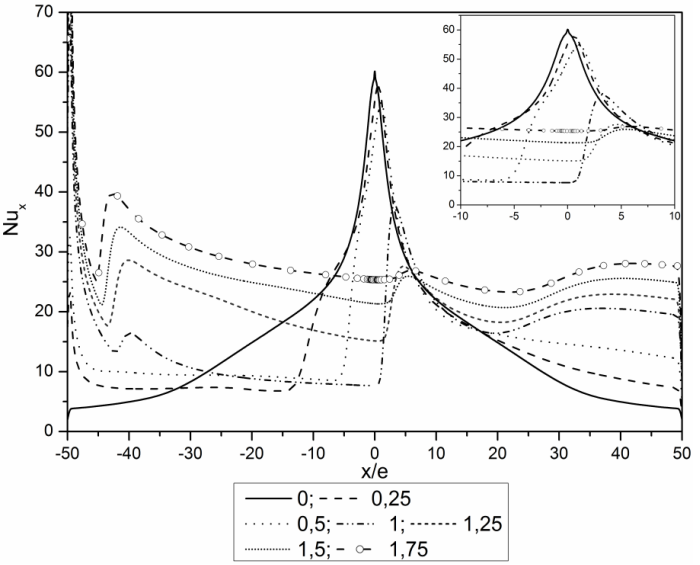

Figure 11: Distribution of local Nusselt number along the hot moving wall for Re=10600 and $0 \leq R_{sj} \leq 1.75$.

Figure (9) shows the evolution of local Nusselt number Nu(x) along the moving plate for Re=10600 and for several values of R_{sj}. It is observed from this figure

that, for stationary plate (R_{sj}=0), the curve is symmetrical, it is characterized by a maximum at the stagnation points which is located on the jet axis. On either side of this axis, the local Nusselt number decreases gradually. For the case of the moving wall $R_{sj} \neq 0$, one notes a peak appears at the left end of the impinging wall (x/e = -50), which augments when R_{sj} increases. The development of this maximum may be explained by the velocity discontinuity between the moving part and the left side immobile wall part [Senter (2006)].

For the cases $0.25 < R_{sj} < 1$:

The optimum value decreases and its position is deflected in the same direction of the moving plate, this is due to the shear generated by plate motion. A drop occurs in the left part of the plate. This reduction is coupled to the generation of the new recirculation [Senter (2006)].The local Nusselt number augments on the right part of the plate when R_{sj} increases by the effect of the progressive jet deviation.

For $R_{sj} > 1$:

For these cases, the plate velocity is greater than that of the jet. The maximum value of local Nusselt number progressively disappears at the left side of the wall. The Nu(x) increases significantly, this is due to the shear generated by the movement of the wall.

3.2.2.2 Effect of surface-to-jet velocities ratio

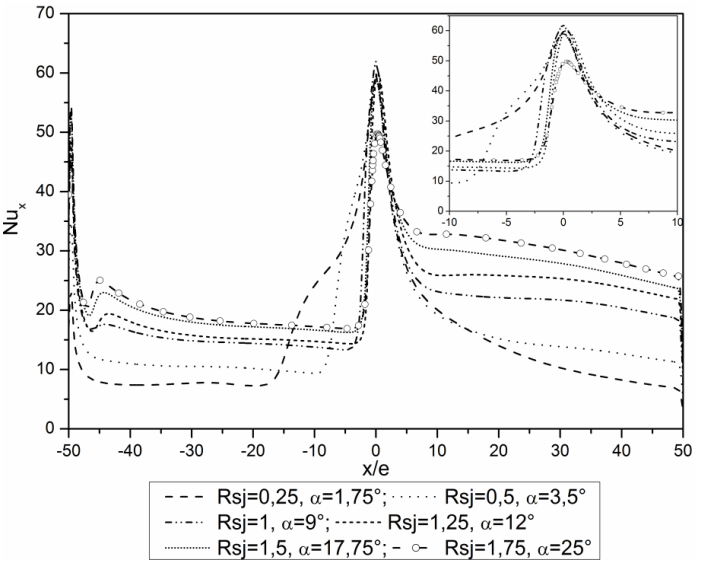

Figure 12: Distribution of local Nusselt number along the hot moving wall for Re=10600, $0 \leq R_{sj} \leq 1.75$ and $0^{\circ} \leq \alpha \leq 25^{\circ}$.

In Figure 11 illustrates the distribution of the local Nusselt number for each surface-to-jet velocity ratio R_{sj}, a It is observed from this figure that, for a stationary plate (R_{sj}=0), the curve is symmetrical, it is characterized by a maximum at the stagnation points which are located on the jet axis. It was found that the inclination of the nozzle increases with increasing surface-to-jet velocities ratio (R_{sj}). The value of the local Nusselt number at the stagnation point increases compared to the case of vertical jet. When the surface-to-jet velocities ratio R_{sj} increases, Table 3 shows the increasing percentage of the stagnation local Nusselt between the two cases (inclined and non-inclined jet).

Table 3: Gain of the stagnation Nusselt number.

R_{sj}	0.25	0.5	0.75	1	1.25	1.5	1.75
$\delta(\%)$	3.884	8.554	//	63.834	116.772	126.759	84.729

Figure (12) shows the evolution of average Nusselt number for Re=10600 according to surface-to-jet velocity ratios between -30e and 30e for the cases of the vertical and inclined jet. One notes from this figure that the optimal inclination of the nozzle of the jet improves the heat transfer. Table 4 represents the gain of the number of average Nusselt between the inclined case and the perpendicular case ($\delta(\%)$). It is observed that it increases when the surface-to-jet velocity ratio increases until Rsj=1.0, then decreases gradually until 0.57% for R_{sj}=1.75.

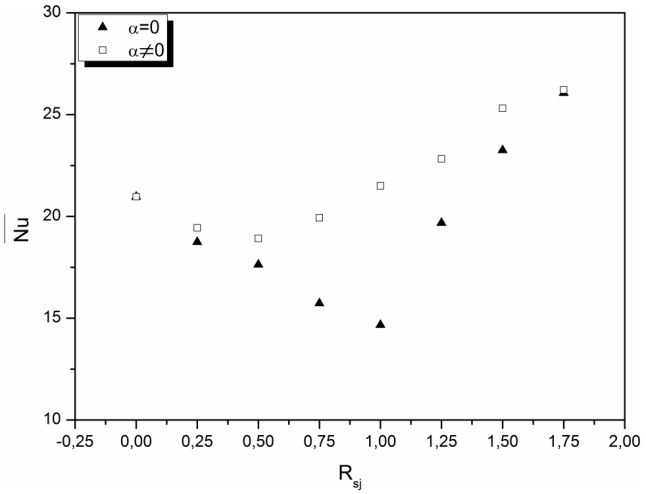

Figure 13: Average of Nusselt Number (α=0° and $\alpha \neq$0°), Re=10600.

Table 4: Gain of the average Nusselt number.

R_{sj}	0.25	0.5	0.75	1	1.25	1.5	1.75
$\Delta(\%)$	3.73	7.31	26.70	46.55	16.00	8.86	0.57

3.2.2.3 Effect of Reynolds number

The effect of Reynolds number on local Nusselt number shows on figure (12), for Reynolds number, ranging from 10000 to 25000 at a given surface-to-jet velocity ratio of R_{sj}=0.75 and 1.25 for vertical and inclined jet case. It is noticed that for the same surface-to-jet velocity ratio:

The local Nusselt number Profile are similar, the displacement of the maximum value is reached at the same point for all the Reynolds within the range of the considered study, the ideal inclination of a nozzle of the jet is the identical but their optimal values increases with the Reynolds number.

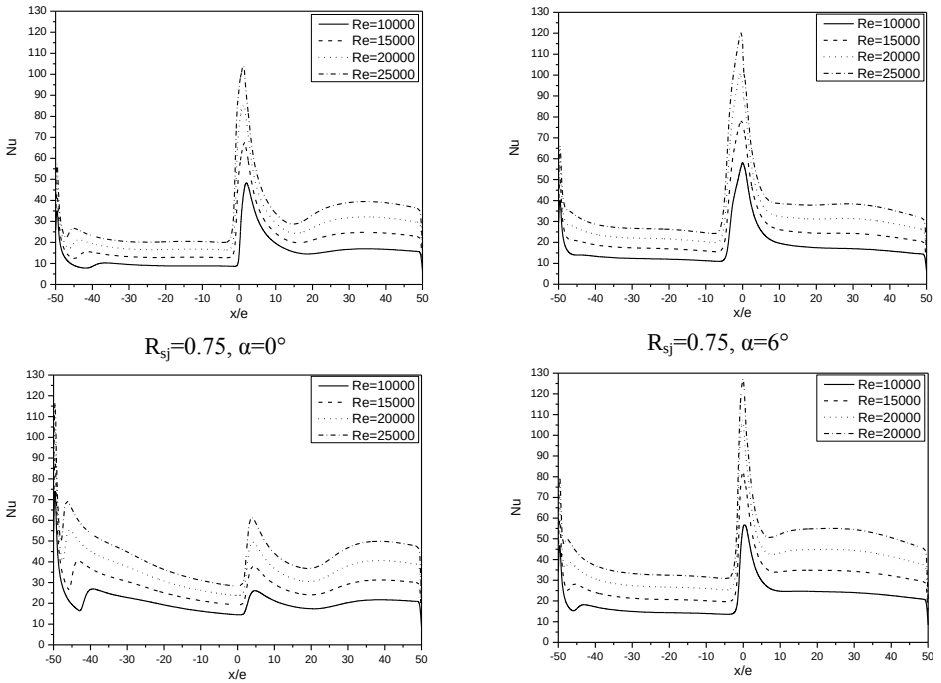

Figure 14: Effect of Reynolds number on local Nusselt number.

3.2.2.4 Correlation of average Nusselt number

Figure 14 (a and b) shows the variation of average Nusselt number according to velocity ratios for Reynolds number range of 10000 to 25000 for the case of vertical and inclined jet, respectively. The average Nusselt number decreases until Rsj=1 (R_{sj}=0.5 for inclined jet) and then increases with surface-to-jet velocities ratio. On the other hand, for a given velocity ratio, the average Nusselt number increases when the Reynolds number is increased.

To conclude, the average Nusselt number evolution according to surface-to-jet velocities ratio and Reynolds number is correlated by the following expressions:

- For the perpendicular interaction (Eq. 7):

$$\begin{aligned} &0 \le R_{sj} \le 1: \quad \overline{Nu} = 0.0065(1 - 0.3760R_{sj} + 0.0604R_{sj}^2)Re^{0.8711} \\ &1 \le R_{sj} \le 1.75: \quad \overline{Nu} = 0.0065(-0.6286 + 1.6504R_{sj} - 0.3387R_{sj}^2)Re^{0.8711} \end{aligned} \tag{7}$$

- For the inclined interaction (Eq. 8), the correlation depends additionally on the inclination:

$$\begin{aligned} &0 \le R_{sj} \le 0.5: \quad \overline{Nu} = (0.0079 - 0.0019R_{sj} + 0.00033R_{sj}^2)Re^{0.851}\cos\alpha \\ &0.5 \le R_{sj} \le 1.75: \quad \overline{Nu} = (0.0068 - 0.00032209R_{sj} + 0.001715R_{sj}^2)Re^{0.851}\cos\alpha \end{aligned} \tag{8}$$

with a scatter of 5%.

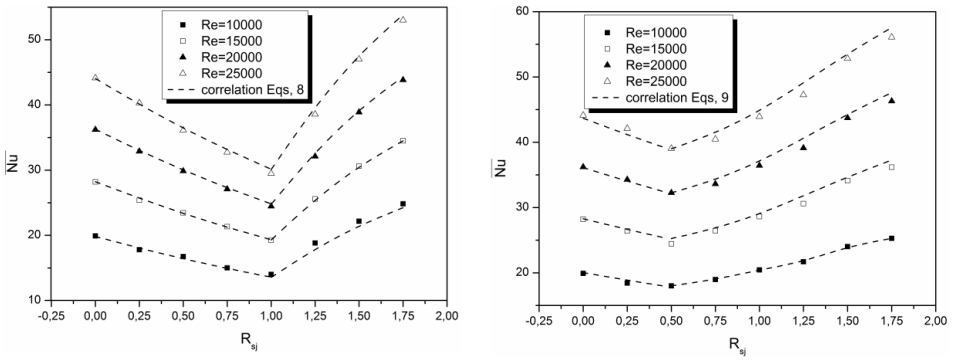

(a) Vertical jet case (b) Inclined jet case

Figure 15: Average Nusselt number distribution with surface-to-jet velocities ratio.

4 Conclusion

The flow structure and resulting heat transfer characteristics related to a confined inclined slot jet impinging on a moving surface have been investigated numerically for different values of the jet exit Reynolds number and surface-to-jet velocities ratio. The RSM turbulence model with enhanced wall treatment for the near wall turbulence modeling has been used.

The main results may be summarized as follows: With increasing surface-to-jet velocities ratio, the magnitude of the maximum local Nusselt number decreases and its position is shifted in the direction of motion of wall. Moreover, for a relatively high velocity of plate the distribution becomes more uniform because the flow is completely detached from the wall.

The average Nusselt number decreases up to Rsj=1, then it increases with an increase in the surface-to-jet velocities ratio (Rsj). However, the inclination of the jet nozzle with an optimal angle in the direction opposite to the motion of the wall considerably improves local heat transfer in the region of the breakpoint. The average Nusselt number is also enhanced, it has a minimum for Rsj = 0.5.

References

Beitelmal, A. H.; Saad, M. A.; Patel, C. D. (2000): The effect of inclination on the transfer between a flat surface and an impinging two-dimensional air jet. *International Journal of Heat and Fluid Flow*, vol. 21, pp. 156-163.

Beltaos, S. (1976): Oblique impingement of plane turbulent jets. *J. of the Hydraulic Division, ASCE*, vol. 109 no. 9, pp. 1177-1192.

Benmouhoub, D.; Mataoui, A. (2013): Turbulent heat transfer from a slot jet impinging on a flate plate. *Journal of Heat Transfer, Transaction of the ASME,* vol. 135, pp. 1-9.

Chattopadhyay, H.; Biswas, G.; Mitra,N. K. (2002): Heat transfer from a moving surface due to impinging slot jets. *Journal of Heat Transfer*, vol. 124, pp. 433–440.

Chattopadhyay, H.; Saha, S. K. (2003): Turbulent heat transfer from a slot jet impinging on a moving plate. *International Journal of Heat and Fluid Flow*, vol. 24, pp. 685–697.

Gardon. R.; Akfirat. J. C. (1966): Heat transfer characteristics of impinging two-dimensional air jets. *Journal of Heat Transfer, Transaction of the ASME*, vol. 88, pp- 101-108.

Huang, P. G.; Mujumdar, A. S.; Douglas, W. J. M. (1984): Numerical prediction of fluid flow and heat transfer under a turbulent impinging slot jet with surface

motion and crossflow. *Transactions of the ASME*, pp. 1-8. Paper 84-WA/HT-33.

Kader, B. (1981): Temperature and concentration profiles in fully turbulent boundary layers. *Int. Heat Mass Transfer*, vol. 24, no. 9, pp. 1541-1544.

Korger, M.; Krizek, F. (1972): Die Stoffubergangszahlen beim aufprall schräger Flächstrablen auf eine platte. *Verfahrenstechnik, Mainz*, vol. 6, no. 7, pp. 223-228.

Launder, B. E.; Reece, G. J.; Rodi, W. (1975): Progress in the Development of a Reynolds-Stress Turbulence Closure. *J. Fluid Mech.*, vol. 68, no. 3, pp. 537-566.

Ramezanpour, A. (2007): A numerical heat transfer study of slot jet impinging on an inclined plate. *International Journal of Numerical Methods for Heat &Fluid flow*, vol. 17, no. 7, pp. 661-676.

Senter, J. (2006): Analyse expérimentale et numérique des écoulements et des transferts de chaleur convectifs produits par un jet plan impactant une plaque plane mobile. *Ph.D. Thesis,* University of Nantes, France.

Sharif, M. A. R.; Banerjee, A. (2009): Numerical analysis of heat transfer due to confined slot-jet impingement on a moving plate. *Applied Thermal Engineering*, vol. 29, pp. 532–540.

Subba Raju, K.; Schlünder, E. U. (1977): Heat transfer between an impinging jet and a continuously moving flat surface. *Wärme-stoffübertr*, vol. 10, pp. 131-136.

Tong, A. Y. (2003): On the impingement heat transfer of an oblique free surface plane jet. *International Journal of Heat and Mass Transfer*, vol. 46, pp. 2077-2085.

Zumbrunnen, D. A. ; Incropera, F. P. ; Viskanta, R. (1992): A laminar boundary layer model of heat transfer due to a nonuniform planar jet impinging on a moving plate. *Wärme-Stoffübertr*, vol. 27, pp. 311–319.